IEEE Access
Multidisciplinary ⋮ Rapid Review ⋮ Open Access Journal

Received May 4, 2021, accepted June 28, 2021, date of publication July 8, 2021, date of current version July 23, 2021.

Digital Object Identifier 10.1109/ACCESS.2021.3095754

Case Study: Variable-Voltage DC Bus With Energy Recovery System for Industrial Plants

ANDRE DOS SANTOS LIMA[1], (Graduate Student Member, IEEE), ADERALDO RICARTE GUEDES[1], EDILSON MINEIRO SA JUNIOR[2], AND FERNANDO LUIZ MARCELO ANTUNES[1], (Member, IEEE)

[1]Department of Electrical Engineering, Federal University of Ceara, Fortaleza 60440-900, Brazil
[2]Department of Electrical Engineering, Federal Institute of Ceara, Sobral 62042-030, Brazil

Corresponding author: Andre Dos Santos Lima (andreslima@sobral.ufc.br)

This work was supported in part by Grendene S/A— a footwear company, in part by the Foundation of Support for Scientific and Technological Development (FUNCAP), in part by the Federal University of Ceara, and in part by the Federal Institute of Ceará–Sobral Campus.

ABSTRACT Direct current (DC) buses and microgrids have drawn significant attention owing to the simple integration of distinct sources and energy storage systems. However, most research efforts refer to the use of DC buses for residential, datacenter, and telecommunications applications rather than manufacturing industry, where processes are controlled by alternating current (AC) motor drivers. This work proposes a novel approach of a DC bus used as primary power supply in manufacturing industrial plants for replacing the traditional AC bus. Unlike most applications, the DC bus voltage presents a variable magnitude and allows energy recovery aiming to improve energy efficiency. This arrangement employs a capacitor bank directly to the DC bus, which is responsible for storing the energy that, otherwise, would be lost during the motor braking. Simulation in PSIM software and experimental results on an industrial plant involving a real polyvinyl chloride (PVC) injection machine supplied directly by the DC bus, in which the voltage varies between 535 V and 600 V, are presented and discussed to validate the proposed approach. The obtained results show that the DC bus does not require a rigid control of the voltage magnitude, thus allowing a reduction of up to 5.05% in energy consumption.

INDEX TERMS DC distribution, direct DC-DC conversion, energy efficiency, industrial plants, kinetic energy recovery, variable DC bus voltage, variable-frequency drives.

I. INTRODUCTION

Since the late 19th century, distinct studies focused on the improvement of efficiency regarding alternating current (AC) transmission and distribution systems have been discussed in the literature and industry. AC systems became more popular than their direct current (DC) counterparts owing to the inherent simplicity in adapting distinct voltage levels associated with the use of transformers and consequent reduced cost. However, with the advent and evolution of power electronics, especially in terms of power semiconductor devices, DC systems have drawn significant attention once again [1]–[6].

DC networks have become quite popular lately owing to the advent of renewable energy conversion systems in electric power generation. With the increasing use of electronics, as more and more equipment is supplied by DC power, significant research effort has been dedicated to the development of DC buses in small-size networks to supply high-power loads and minimize losses [7]. A thorough review on DC power systems is presented in [6], focused on traditional applications, e.g., data centers, space stations, traction systems, and large ships. Low-voltage DC systems associated with distributed generation and integrated with AC buses are proposed as an alternative to the traditional AC systems in [8]–[12].

DC power has been traditionally used in telecommunications systems for both data and voice transmission. Lawrence Berkeley National Lab started researching DC power systems in 2004, also investigating the use of power supplies and uninterruptible power systems (UPSs) in telecom equipment aiming to reduce losses due to redundant power conversion stages. The use of a 380-V DC bus was then proposed so that the loads could be directly supplied through DC-DC

The associate editor coordinating the review of this manuscript and approving it for publication was Jonathan Rodriguez.

converters. As a result, efficiency was increased by 28% in datacenters where the DC bus was formerly obtained from AC-DC converters responsible for providing DC voltages from the AC grid rated at 220/380 V [13]–[16]. EMerge Alliance, an open industry association of energy and telecommunication equipment manufacturers, was created to promote research and development of standards focused on energy efficiency in the context of data center equipment and residential applications where DC buses are employed. It is worth mentioning that the development of a standard for the use of 380-V DC buses in datacenters and telecom applications is currently in progress [17]–[21].

In new recent research performed by Lawrence Berkeley National Lab, economic studies have proven that replacing an AC bus with a DC one is quite advantageous. Energy efficiency studies in industrial systems and commercial buildings have demonstrated that the use of DC buses leads to improved performance as claimed in [22]–[31], although no results are shown when it comes to industrial plants. New standards and the normalization of voltage levels, as well as safety and protection issues, are still the main challenges for the widespread use of DC buses according to [32].

Traditionally, the local AC grid presents fixed frequency and voltage magnitude to achieve stability. The same rules apply to DC bus voltages, which are often assumed to present constant voltages as obtained from power electronic converters. These buses also have strict voltage magnitude control, with low ripple [28], [33]. Since 2004, when the Berkeley National Lab started working on DC buses for buildings, researchers have focused on the conception of fixed-voltage buses with distinct levels for specific applications as seen in [34]–[36].

Many industrial applications like elevators, machining centers, wood cutting, packaging, plastic injection molding, forming presses, forklifts, robots, and sewing require electric machines operating in an intermittent regime and, in some cases, short-time operating cycles. With the frequent acceleration and deceleration, there is the possibility of energy recovery by converting the kinetic energy associated with such manufacturing processes into electric energy.

The braking process of an electric motor connected to a driver can cause variations in the voltage magnitude of the internal DC link of the power converter. The energy recovery associated with the braking process has been thoroughly studied in the context of electric vehicles (EVs) in [37], as well the optimization of DC buses in [38].

As a contribution to this field, this work proposes the use of a variable-voltage DC bus for a manufacturing industrial plant instead of using a constant-frequency, constant-voltage AC bus. The advantages lie in the fact that there is no need for a rigid control of the DC bus voltage, with an extra feature of eliminating the internal rectifier of every motor driver, thus improving the overall efficiency.

The proposed DC bus has a lower limit of the voltage magnitude to ensure motor starting, whereas the magnitude can increase to a higher level to preserve the existing electronic components. The energy surplus of the DC bus due to the braking of motors can be stored in capacitor banks directly connected to the bus. The effectiveness of the proposed variable-voltage system is validated through simulation and experimental results in a real footwear manufacturing plant.

II. DC BUS USED IN INDUSTRIAL MOTOR DRIVE APPLICATIONS

Increasing the efficiency of motor drives and related systems is of major importance because 40% of the electric energy generated worldwide is consumed by electric motors in industry [39], [40]. In this context, the replacement of induction motors (IMs) with permanent-magnet synchronous motors (PMSMs) was addressed in [41], [42]. With the significant advances in power electronics, the amount of PMSMs driven by inverters has increased significantly, mainly because the cost associated with drivers has become competitive with their three-phase IM counterparts as shown in Fig. 1. Commercially-available inverters allow the variable-frequency operation aiming at speed control so that the motor efficiency is as high as possible [39], [43]. Inverter-based motor drivers have become more efficient without loss of robustness as demanded by industrial environments, as the associated control systems are able to drive both IMs and PMSMs [44], [45]. However, most inverters available in the market require a DC bus composed of an uncontrolled rectifier followed by an output low-pass filter, as such AC-DC converter is directly connected to the AC grid. The DC bus voltage typically varies within a specific range. To limit the maximum DC bus voltage, a dissipative protection circuit is often used to maintain the voltage within safe values supported by the semiconductor devices. Most inverter losses are due to uncontrolled rectifiers and dissipative protection devices. Regenerative inverter drives are uncommon in industry applications, as well the use of bidirectional rectifiers as studied in [46]–[49].

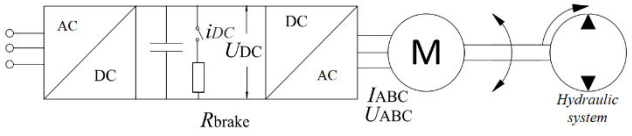

FIGURE 1. Motor connected to a three phase AC bus through an inverter.

The use of variable-voltage DC buses becomes more advantageous for replacing the traditional three-phase AC grid in motor drives. In this case, there is the direct integration between the DC bus and the inverters, with the possibility of energy recovery during braking using capacitor banks, or even other machines connected to the same DC bus. Besides, there is a wide variety of possible applications, e.g., the integration of renewable energy sources such as solar and wind [50], as well as the reduction of the number of power conversion stages.

Two wires are typically used in DC distribution systems, but three wires may also be used if symmetrical voltages are required. Reduced cabling needs is one of the main advantages associated with DC systems, thus leading to lower cost in terms of infrastructure. Unlike AC grids, there is no reactive power flow. Therefore, the resulting losses are only due to the currents flowing through the conductor material, and there are no losses associated with harmonics.

In this context, this work proposes the use of a DC bus as a primary power supply to the industrial plant based on an energy recovery system. The rectifiers used to build the whole industrial DC bus are not studied in this work. Fig.2 shows a schematic of the proposed arrangement with inverters and a capacitor bank directly connected to the DC bus. Thus, it is possible to avoid the use of internal rectifiers, implying a reduced number of power conversion stages. In this study, the DC bus is always present as a premise. The DC bus voltage can vary with the amount of kinetic energy recovered from the motors, while also ensuring the safe operation of semiconductors and cable insulation.

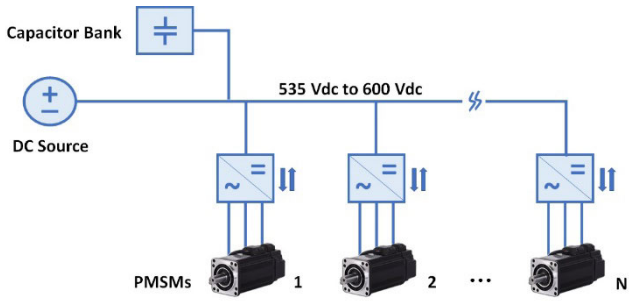

FIGURE 2. Motors connected to DC bus using sinusoidal pulse width modulation (SPWM) inverters.

Besides, there is no defined control strategy to coordinate energy changes between the energy recovery system and motor drivers. The energy transfer occurs randomly and depends on the amount of energy that can be recovered while the motor is braking or the consumption by another motor during a new starting. There is no synchronous operation between different injection molding machines, they are semiautomated and totally independent. The DC bus should be robust enough to support the starting of motors without compromising the stability.

Since the machines are associated with independent processes, it is not necessary to employ multi-motor drive system techniques commonly used to control a sequential process with many units. The authors in [51] propose a technique that uses high-gain observers together with state feedback control to obtain a separation principle for the stable operation of the whole system. This approach has proven to be suitable for a belt tension with a multi-motor driver. In another work [52], the authors present an AC multi-motor drive system based on a common DC bus for energy regeneration. The system characteristics are thoroughly assessed, whereas a model is derived for the representation of discrete-event dynamic systems. This kind of structure involves a soft energy transfer process that can be predicted by the control system aiming at better absorbing the exceeding energy.

III. SIMULATION OF ENERGY CHANGES AMONG MOTORS AND DC BUSES

In manufacturing industry, the breaking and acceleration processes of several machines are frequent. During braking, the kinetic energy stored in the machine rotor must be dissipated by mechanical brakes, or electronic systems that convert most energy into heat using resistors. High losses exist in this condition, which increase as the machine is further accelerated and decelerated during many operating cycles.

It is necessary to perform proper measurements to define the amount of energy involved in the entire process, as well as to propose alternatives for recovering it aiming at later use. In order to simulate an industrial process, a hydraulic pump associated with a plastic injection machine was chosen in this study. This is because this process involves the frequent motor starting and stopping, in which it is possible to recover energy based on an efficient approach.

A. ELECTRO-HYDRAULIC SIMPLIFIED MODEL

In an injection process, the pressure must be controlled to inject polyvinyl chloride (PVC) material into the mold. The servo driver that controls the PMSM receives signals of pressure and flow from the injection molding machine controller to set the motor speed. At the set pressure, the motor does not stop at all and maintains a certain speed to ensure that the system does achieve the required pressure. Fig. 3 shows the block diagram of the PMSM control system in an injection molding machine. The PMSM is controlled by two signals from an internal resolver and a pressure sensor located at the hydraulic system.

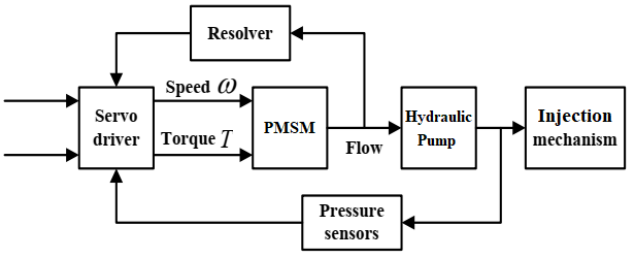

FIGURE 3. Block diagram of the PMSM control system in an injection molding machine.

The kinetic energy that can be recovered from this electro-hydraulic system depends directly on the motor speed, considering the hydraulic system as an inertial load and neglecting the oil damping. Thus, the kinetic energy variation available in the deceleration of a motorized system can be defined by (1).

$$\Delta E_k = \frac{1}{2} \cdot J_t \cdot \left(\omega_{r_{initial}}^2 - \omega_{r_{final}}^2 \right) \tag{1}$$

where ΔE_k is the kinetic energy variation during the motor deceleration; J is the total moment of inertia of the system; $\omega^2_{r\_initial}$ is the initial rotor speed (deceleration start); and $\omega^2_{r\_final}$ is the final rotor speed (deceleration stop).

In systems with higher moments of inertia and depending on the amount of stored energy, the deceleration time and the dissipated energy may be high and, consequently, the overall system efficiency may be reduced. The total moment of inertia of the system is due to the motor, the mechanical coupling, and the hydraulic pump as expressed by (2).

$$J_t = J_{motor} + J_{coupling} + J_{Pump} \tag{2}$$

The mechanical equation of the motor can be expressed by (3). It is worth mentioning that the moment of inertia of the coupling between the motor and pump was neglected because it has a low mass and diameter.

$$T_e - T_L = J\frac{d_\omega}{d_t} + B\omega \tag{3}$$

According to [53]–[55], it is extremely complex to represent the losses in a hydraulic system based on a mathematical approach, since the characteristics of the oil present in these systems change significantly with the temperature. Thus, an approximation can be made considering the hydraulic part as a load with an inertial component. The kinetic energy stored in the electric machine during the deceleration of the motor cannot be totally recovered in the form of electric power, because there are some losses, namely mechanical and electrical ones.

The mechanical losses are caused by the motor friction and the portion of kinetic energy consumed by the mechanical load during deceleration, as well as the hydraulic fluid of the pump. The electrical losses are associated with the motor, the inverter, and the bidirectional power electronic converter. The final amount of recoverable kinetic energy in a motor can be estimated if all mechanical and electrical losses are calculated and subtracted from the generated kinetic energy according to (4) [54], [56], [57].

$$E_{kutil} = \Delta E_k - E_{P\_mec} - E_{P\_mot} - E_{P\_inv} - E_{P\_con} \tag{4}$$

where E_{kutil} is the recoverable amount of useful energy; E_{P_mec} represent the system mechanical losses; E_{P_mot} corresponds to the motor electrical losses; E_{P_inv} denotes the inverter losses; and E_{P_con} is the bidirectional converter losses.

According to simulation tests performed by [58] and [59], in a PVC injection process, depending on the load size and production cycle, up to 49% of the energy lost by an injection molding process can be stored in supercapacitors. The kinetic energy lost in the industrial process can be converted to electric energy and increase the voltage across the DC bus of the motor driver using clamping resistors to protect semiconductors.

B. SIMPLIFIED MODEL, DESIGN, AND SIMULATION

Two scenarios are analyzed using PSIM®software to show the power flowing through the DC bus, which involves two motor drivers and the energy storage system similarly to Fig. 2. The specifications of PMSMs are listed in Table 1, considering a rated load torque of 64 N·m to emulate the operation of the hydraulic pump of an injection molding machine. The motors and the energy recovery system composed of a capacitor bank are connected to the DC bus.

TABLE 1. Parameters of the PMSM used in the simulation.

Simulation Data	
R_s (stator resistance) [Ω]	0.27
L_d. (d-axis inductance) [H]	4.41 m
L_q (q-axis) inductance [H]	4.41 m
$V_{pk}/kRPM$ (line-to-line peak voltage/1000 rpm)	200 V/$kRPM$
Number of poles	8
Moment of inertia [kg·m^2]	0.012
Shaft time constant	10

The capacitance of the energy storage system is greater than those of the motor drivers and was designed to absorb the energy from the braking, which can be calculated from (5).

$$E_{d\_br} = \int_0^t P_d \cdot t \tag{5}$$

where E_{d_br} is the energy lost during the braking (J); P_d is the power dissipated during the braking (W); and t is the time interval representing the actuation of the braking protection system.

It is possible to design a capacitor bank to store the dissipated energy for later use according to (6).

$$C = \frac{2 \cdot E_{reg\_max} \cdot N_{motors}}{V^2_{bar\_max} - V^2_{bar\_min}} \tag{6}$$

where E_{reg_max} is the energy recovered during the longest braking session; N_{motors} is the average number of motors that are decelerated simultaneously; V_{bar_max} is the maximum voltage across the DC bus; and V_{bar_min} is the minimum voltage across the DC bus.

Fig. 4 shows the voltage increase on the capacitor of the motor driver that is directly connected to the DC bus. In this condition, the capacitor is charged by the excess of energy provided by the DC bus. This voltage variation is used to design the capacitor bank of the recovery system.

1) ONE MOTOR BRAKING AND ONE MOTOR ON FULL LOAD

Fig. 5 shows the power flow in the DC bus as the result of a PMSM braking. There are two motors connected to the DC bus. The first one is braking and the second one is on full load. According to curve *Pmotor_1* in blue, it is possible to obverse the moment at which the motor stops. Then it starts operating as a generator owing to the kinetic stored in the shaft, as the power flows to the DC bus, charging the capacitor bank and increasing the DC bus voltage as a consequence.

The power peak in the blue curve can be explained by the elastic force on the freewheel movement. The green curve *Pmotor_2* shows the behavior of the second motor driver when there is an instantaneous increase of energy. On the other hand, the power provided the primary DC source

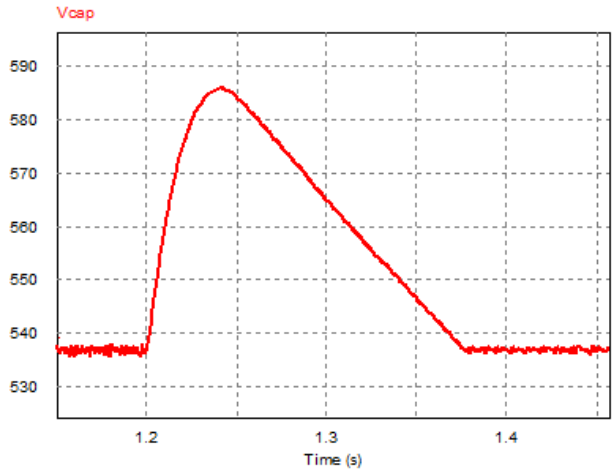

FIGURE 4. Voltage increases on the capacitor of the motor driver.

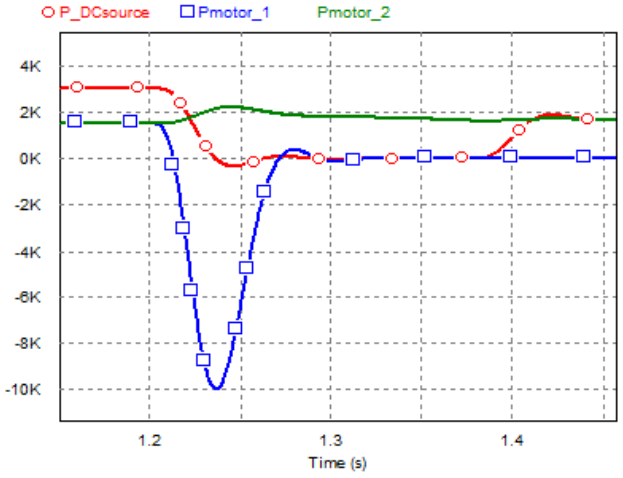

FIGURE 5. Power flow between two motors with one motor braking and one motor on full-load condition.

P_DCsource decreases because of the energy recovered by the first motor. If any recovery system is connected to the bus, an overvoltage protection system must be enabled to dissipate the excessive energy and protect the power converters.

2) 1st. ONE MOTOR DECELERATING AND ACCELERATING, WITH ANOTHER MOTOR DISCONNECTED

In this scenario represented by Fig. 6, the second motor is disconnected from the DC bus and the first one does not stop at all. The first motor driver is disconnected and then connected again. As expected, the machine operates as a generator while braking, and the capacitor bank is charged as a consequence. The power absorbed from the DC bus corresponding to *P_DCsource* bus becomes nearly null. Thus, the remaining portion of kinetic energy is transferred to the capacitor bank according to the behavior of curve *Pmotor_1* in Fig. 6, which becomes negative. After that, the motor accelerates again and starts consuming the energy previously stored in the DC bus.

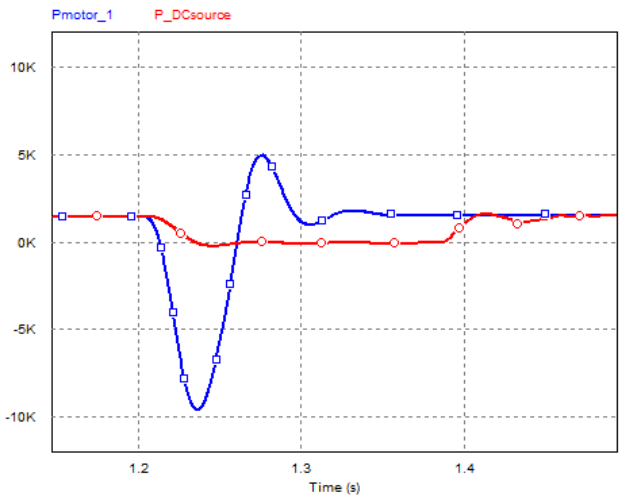

FIGURE 6. Power flow between motor 1 and the DC bus while it decelerates and accelerates again.

In this simulation, the power flow between the machines connected to a same DC bus may assume distinct characteristics depending on the actual number of parallel-connected machines. Since the load has a high inertia moment and the simulation period is short, the speed does not vary significatively. However, some energy could still be recovered and supplied to the DC bus.

IV. EXPERIMENT PERFORMED ON A FACTORY

The first experimental test was carried out to analyze the power flow and the increase of the DC bus voltage associated with the manufacturing process, so that accurate data could be collected for the proper design of the capacitor bank.

The tests were performed in an industrial environment with two types of injection molding machines, that is, models GEK 220/S and GEK 280/S by Golden Eagle. The voltage and current levels required to determine the amount of energy involved in the starting and braking processes were then measured, considering the machine operation while producing small PVC parts. It is worth mentioning that there was no external interference in the production process during the acquired experimental data. The injection molding machine can be seen in Fig. 7.

Tables 2 and 3 show the parameters of the PMSMs and inverters, where PMSM 1 and PMSM 2 are driven by inverter 1 and inverter 2, respectively. PMSM 1 and PMSM 2 are associated with the machine models Golden Eagle GEK 220/S and Golden Eagle GEK 280/S, respectively.

All measurements and curves were obtained using an oscilloscope model DPO3014, current probes model TCP303, high-voltage differential probes model P5200 by Tektroniks, and an energy analyzer model RE6000 by Embrasul.

Fig. 8 shows the experimental setup, where *Vbar* is the voltage across the DC bus measured at point (5), and *Vrf* is the voltage across the braking resistor measured at point (2). The current probes were connected at points (4) and (3) to

TABLE 2. Parameters of the PMSMs.

Parameters	PMSM 1	PMSM 2
Manufacturer / Model	Phase/U31007F20.3	Phase/U31010F18.3
Rated power	18.71 kW	23 kW
Efficiency	92%	95%
Rated torque	89.39 N·m	122 N·m
Rated speed	2,000 rpm	1,800 rpm
Rated current	36.67 A	44 A
Rated voltage	341 V	321 V
Constant torque	2.53 N·m/A	2.9 N·m/A
Rated frequency	113 Hz	113 Hz
Winding resistance	0.46 Ω	0.27 Ω
Winding inductance	11.40 mH	5.41 mH
Rotor inertia	0.009 kg·m²	0.012 kg·m²
Number of poles	8	8
Weight	52 kg	66 kg

FIGURE 7. Measurement instruments associated with the plastic injection molding machine in a footwear factory.

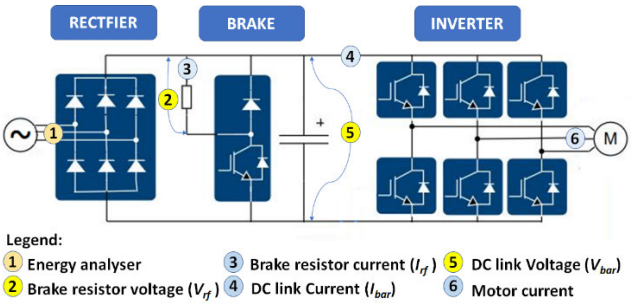

FIGURE 8. Voltage and current probes employed in the motor drive system.

measure *Ibar* (DC bus current) and *Irf* (current through the braking resistor), respectively.

The injection machine was configured according to proper parameters for the injection molding process as established by the company depending on the requested mold.

TABLE 3. Parameters of the inverters used in the experiment.

Inverters	Inverter 1	Inverter 2
Manufacturer / Model	Focal/F8N3T0022	Delta/VDF300V L43B–J
Rated power	23 kW	23 kW
Rated voltage	380 V	380 V
DC-link capacitance	3.3 mF	3.5 mF
Maximum DC bus voltage*	800 V	800 V
Maximum DC bus current*	200 A	200 A
Voltage limit for the actuation of the braking resistor	590 V – 610 V	600 V
Braking resistor	30 Ω	30 Ω

Measurements were performed to determine how much power is demanded at each second over the entire cycle of material injection. This is important for the development of any power converter that may be employed to allow the energy exchange between the machines and the DC bus. It is also worth mentioning that each injection cycle lasts about 16 seconds.

Fig. 9 shows the acquired results in terms of the power curve for one cycle of the injection process. The red curve represents the overall power measured at point 1 in Fig. 8. The blue curve corresponds to the power measured at point 5 after the rectifier. It is observed that the higher power demand occurs during the molding stage. From the power dissipated in the protection resistor, as well as the maximum and minimum voltages across the DC link of the inverter, it is possible to determine how much energy can be recovered in the process. The amount of dissipated energy in the resistor during the braking process of the motor in machine GEK 220/S was carried out using the mathematical function of the oscilloscope during one operating cycle. The result was also confirmed after the comma-separated values (CSV) file was generated from the data acquisition. Thus, the average power could be calculated by the oscilloscope, as the amount of energy dissipated in the braking resistor could be determined for each step of the process.

Fig. 10 shows experimental results regarding the current and voltage measured in the inverter of the injection molding machine for a complete cycle of about 16 s. It is worth mentioning that the braking system consists of a resistor connected to a switch in parallel with the DC link of the motor driver. The circuit is activated when the voltage across the DC link reaches a given desired value.

The motor was braked five times during the operating cycle (F1, F2, F3, F4, and F5), but the breaking resistor did only act during F2 and F5. During F3, the motor decelerates, but before its stops totally it is driven again as the voltage limit required to enable the protection system is not reached. The energy regenerated by the motor is then absorbed by the DC bus.

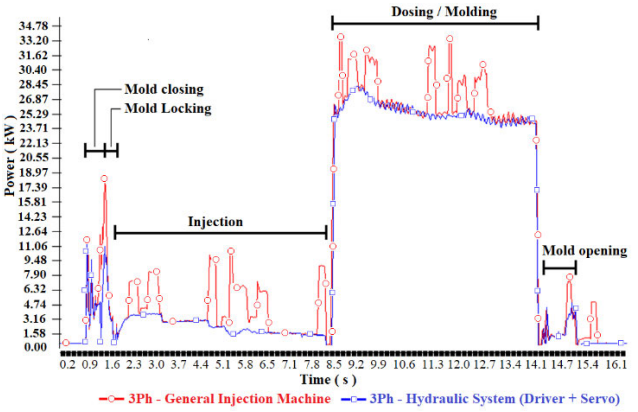

FIGURE 9. Power measurement for one cycle of the injection process: power measured at the main input (red) and power measured at the motor driver input (red).

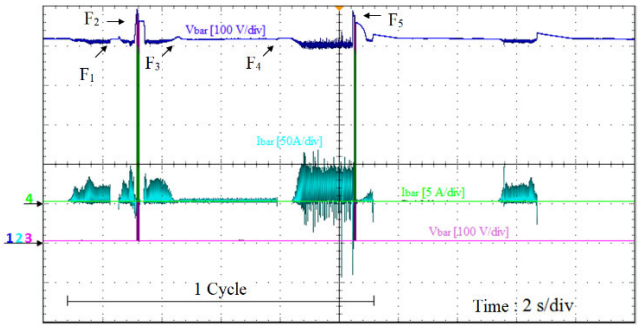

FIGURE 10. Experimental results for one operating cycle: Ch 1 (100 V/div. – dark blue) – DC bus voltage (*Vbar*), Ch 2 (50 A/div. – light blue) – DC bus current (*Ibar*), Ch3 (100 V/div. – pink) – voltage across the braking resistor (*Vrf*), and Ch 4 (5 A/div. – green) – current through the braking resistor (*Irf*). Time scale: (2 s/div).

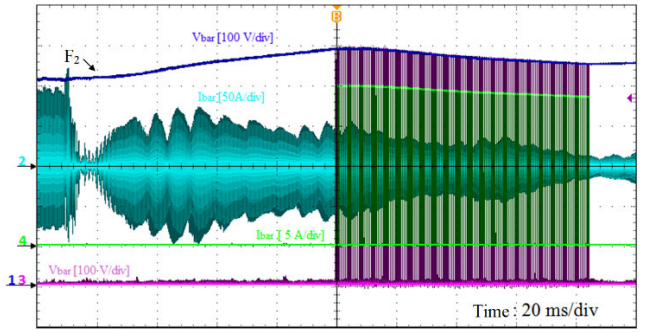

FIGURE 11. Experimental results for the second deceleration session of the motor: Ch 1 (100 V/div. – dark blue) – DC bus voltage (*Vbar*), Ch 2 (50 A/div. – light blue) – DC bus current (*Ibar*), Ch3 (100 V/div. – pink) – voltage across the braking resistor (Vrf), and Ch 4 (5 A/div. – green) – current through the braking resistor (*Irf*). Time scale: (20 ms/div).

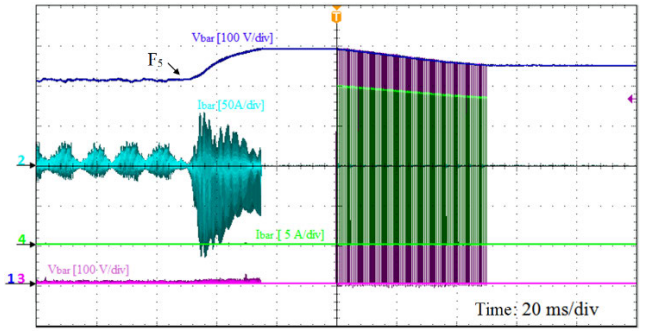

FIGURE 12. Experimental results for the fifth deceleration session of the motor: Ch 1 (100 V/div. – dark blue) – DC bus voltage (*Vbar*), Ch 2 (50 A/div. – light blue) – DC bus current (*Ibar*), Ch3 (100 V/div. – pink) – voltage across the braking resistor (*Vrf*), and Ch 4 (5 A/div. – green) – current through the braking resistor (*Irf*). Time scale: (20 ms/div).

During F1 and F4, the motor decelerates, but the kinetic energy is dissipated by the mechanical load itself, i.e., it is damped by the hydraulic pump. During F2 and F5, the DC bus voltage increases by more than 10%, as the braking system protection is activated twice. The DC bus voltage varies when the motor decelerates, causing it to behave as a generator while supplying power to the DC bus.

To calculate the amount of energy dissipated by the breaking resistor, the first actuation of the braking system is considered, which lasts approximately 85 ms according to Fig. 11. During F_2, the maximum voltage across the DC bus is 594.7 V, which is reduced owing to the power dissipated in the braking resistor, thus causing the loss of part of the energy during the PMSM braking. The braking system remains activated until the maximum DC bus voltage reaches the rated value.

Fig. 12 represents the second braking session. During F5, the DC bus voltage increases to 593 V, as it is necessary to connect the braking system to the circuit once again, although the time interval is shorter than 50 ms in this case. The average power calculated by the oscilloscope in the second and fifth braking sessions is 780.7 W and 383.2 W, respectively. Considering an interval of 200 ms defined by oscilloscope window, the dissipated energy can be estimated from (6), resulting in 156.14 J and 76.44 J, respectively.

The total energy dissipated in the braking resistor during a production cycle of about 16 s and with an injection load of approximately 210 g is 232.58 J. If the operation occurs during one hour, 225 cycles result. Therefore, the energy dissipated in the braking resistor is 52.33 kJ. Considering a machine that operates 22 hours a day and six days a week on average under the conditions employed in the experiment, the energy dissipated in the braking resistor over one month will be 27.6 MJ, which is equivalent to 7.7 kWh.

V. ENERGY RECOVERY SYSTEM: DESIGNING THE CAPACITOR BANK

It is possible to implement the variable-voltage DC bus represented in Fig. 2 for a finite number of machines depending on the motor group size. The capacitor bank required to store the dissipated energy was calculated by (6). The maximum voltage across the DC bus is $V_{bar\_max} = 600$ V, whereas the minimum voltage across the DC bus is set to $V_{bar\_min} = 530$ V.

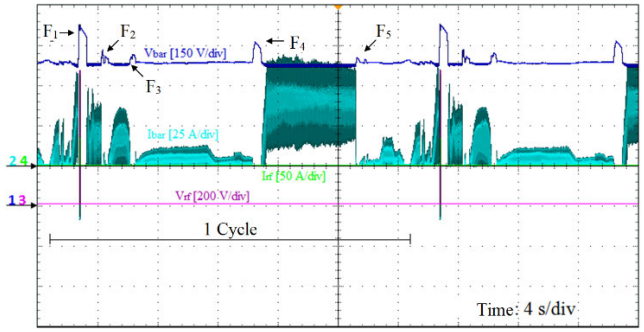

FIGURE 13. Experimental results for one operating cycle without employing the capacitor bank: Ch 1 (150 V/div. – dark blue) – DC bus voltage (*Vbar*), Ch 2 (25 A/div. – light blue) – DC bus current (Ibar), Ch3 (200 V/div. – pink) – voltage across the braking resistor (*Vrf*), *and* Ch 4 (50 A/div. – green) – current through the braking resistor (*Irf*). Time scale: (4 s/div).

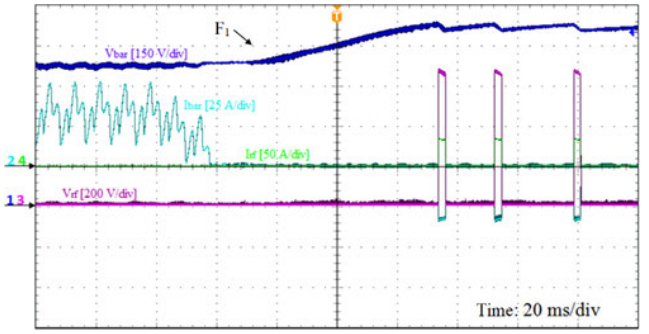

FIGURE 14. Detailed view of the first deceleration session of the motor without employing the capacitor bank: Ch 1 (150 V/div. – dark blue) – DC bus voltage (*Vbar*), Ch 2 (25 A/div. – light blue) – DC bus current (*Ibar*), Ch3 (200 V/div. – pink) – voltage across the braking resistor (*Vrf*), and Ch 4 (50 A/div. – green) – current through the braking resistor (*Irf*). Time scale: (20 ms/div).

The energy recovery system employing a capacitor connected in parallel with the DC bus is typically embedded in commercial inverters to mitigate sudden voltage fluctuations, this being similar to the ones typically employed in EVs. However, the difference lies in the fact that EVs also have internal batteries for energy storage.

According to [37], the capacitor bank must be connected directly to the DC bus, as it allows supplying additional energy demands without the need of a power converter to process the energy stored in the capacitors. Overall, it is reasonable to state that keeping a constant voltage across the supercapacitor to help the batteries during an eventual peak demand is quite inefficient.

Thus, the use of a converter to manage a large amount of energy in a short period of time is a challenging task. The power flow involved in the injection process shown in Fig. 9 involved peaks of 33 kW at 600 V, this being a good reason to connect the capacitor bank directly to the DC bus aiming to avoid converter losses. Other motivation is that the voltage assumes variable values over a wide operating range. The capacitor bank was then designed considering the power flow between motor and driver in the industrial environment. Table 4 lists the parameters adopted in the calculation of the capacitor bank.

TABLE 4. Parameters for the design of the capacitor bank.

Parameter	Value
Minimum DC bus voltage	530 V
Maximum DC bus voltage	600 V
Capacitance	7.9 mF
Number of motors	2

The capacitors employed in the experiment in the industrial plant are part number B43584 by Epcos. The capacitance was calculated from (6) and the measurements performed on the injection machine shown in Fig. 11 and Fig 12,

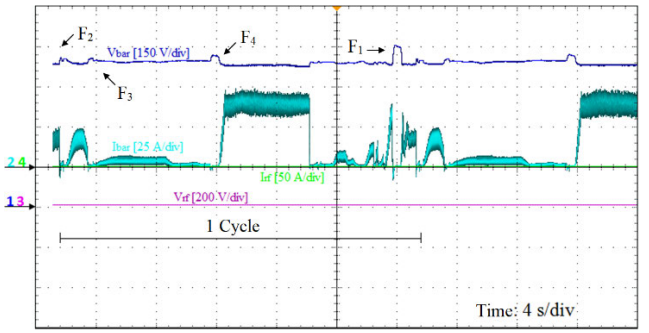

FIGURE 15. Experimental results for one operating cycle employing the capacitor bank: Ch 1 (150 V/div. – dark blue) – DC bus voltage (Vbar), Ch 2 (25 A/div. – light blue) – DC bus current (Ibar), Ch3 (200 V/div. – pink) – voltage across the braking resistor (Vrf), and Ch 4 (50 A/div. – green) – current through the braking resistor (Irf). Time scale: (4 s/div).

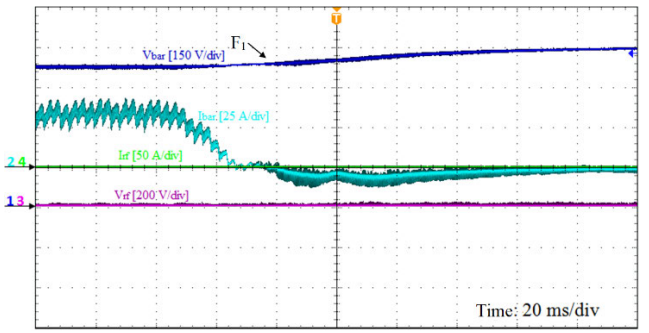

FIGURE 16. Detailed view of the first deceleration session of the motor employing the capacitor bank: Ch 1 (150 V/div. – dark blue) – DC bus voltage (*Vbar*), Ch 2 (25 A/div. – light blue) – DC bus current (*Ibar*), Ch3 (200 V/div. – pink) – voltage across the braking resistor (*Vrf*), and Ch 4 (50 A/div. – green) – current through the braking resistor (*Irf*). Time scale: (20 ms/div).

resulting in 7.9 mF. To obtain the equivalent capacitor associated with the required DC bus voltage, a bank with five parallel-connected branches composed of two series-connected capacitors rated at 3300 μF/400 V was employed, resulting in an equivalent capacitance of 8.25 mF, which is slightly higher than the calculated value.

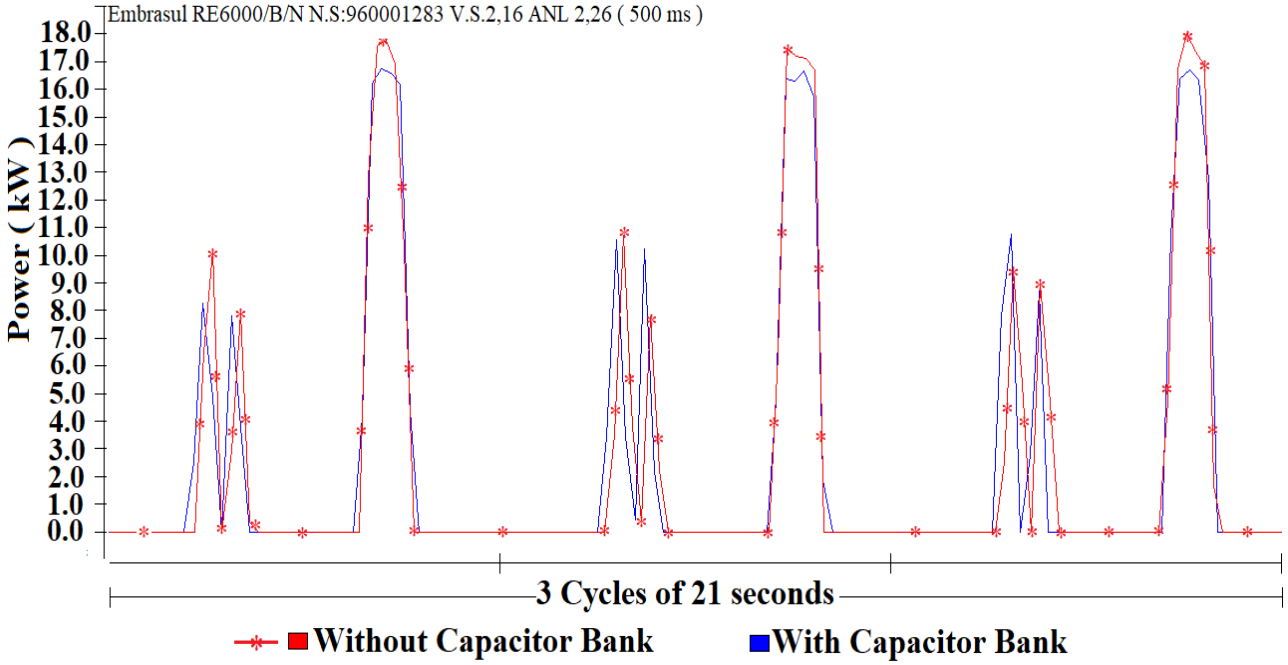

FIGURE 17. Comparison between the active power curves during three cycles (red – without capacitor bank; blue– with capacitor bank).

VI. MEASUREMENTS PERFORMED ON A MACHINE OPERATING IN THE INDUSTRIAL ENVIRONMENT

Owing to the production schedule of the footwear company, the injection machines model GEK 220/S were not available at the moment of the experiment. Thus, experimental data were acquired from another machine with a slightly higher power, i.e., model GEK 280/S, which uses 23-kW PMSMs.

The complete production cycle associated with the experiment lasts approximately 24 s, with an injection load of 170g. The current and voltage were measured to verify the behavior of the DC bus, first without the capacitors connected to it, and then with the capacitor bank connected to the DC bus. It is worth mentioning that the internal capacitance of the motor driver was neglected in the calculation of the total capacitance and was not removed when adding the energy recovery system.

A. MACHINE OPERATING WITHOUT THE CAPACITOR BANK

During the operating cycle In Fig. 13, the motor is braked five times (F1 to F5). However, the braking resistor actuates only during F1. During the remaining ones, the PMSG only decelerates, accelerates again, and then stops. The exceeding energy resulting from the motor deceleration increases the bus voltage, which becomes higher than the maximum limit, causing the braking system to be activated. The bus voltage *Vbar* increases from 528.4 V to 686.2 V, while the average current *Ibar* is 69.66 A. The current waveform in light blue has a high ripple during the whole process as well.

Fig. 14 represents the detailed view of the moment when the motor decelerates. The DC bus voltage *Vbar* increases from 537 Vdc to 670 Vdc very fast, as the protection system must be activated to avoid damage. Besides, voltage *Vrf* corresponds to the voltage across the protection resistor, which is turned on and off by a pulse width modulation (PWM) scheme to keep the average DC bus voltage within safe limits. The exceeding amount of energy is then dissipated by the braking resistor. Thus, it causes a fast variation in the DC bus voltage, thus affecting the motor driver connected to the DC bus.

B. MACHINE OPERATING WITH THE CAPACITOR BANK

In the second experiment, the capacitor bank is connected to the DC bus, whereas the currents and voltages are once again measured as seen in Fig. 15. Unlike Fig.13, voltage *Vbar* at F1 goes from 537 Vdc to 600 Vdc and does not reach the maximum limit set to protect the motor drive. The capacitor bank operates as a peak-shaving system, while it stores the bus energy without affecting the motor driver.

Fig. 16 shows a detailed view of the currents and voltages during the first deceleration session when using the capacitor bank connected to the DC bus. The bus voltage varies more smoothly, reaching 600 V. The braking system is not activated because the voltage level is within safe limits for the motor driver. Current *Ibar* decreases and inverts its direction, thus indicating that the capacitor bank stores energy. If more machines were connected to the bus, the remaining energy could be used instead. As the minimum DC bus voltage required to start the motors is 537 Vdc, it will increase from this value to a maximum limit defined by the protection system of the motor driver. Therefore, the higher the voltage,

the lower the average current through the motor driver, resulting in higher energy efficiency.

During the whole experiment that lasted about 4 hours using machine model GEK 280/S to produce 170g PVC parts, a power analyzer was connected to the AC grid that supplies the diode rectifier for the measurement of consumed power and energy according to the schematic shown in Fig. 8. A large dataset was recorded during this acquisition period. A comparative plot regarding the active power profile of the machine over a period of three cycles equivalent to 21 s each is presented in Fig. 17.

The curves show the active power behavior with and without using the capacitor bank connected to the DC bus. The average amount of energy consumed with and without using the capacitor bank was measured as 6.21 kWh and 6.54 kWh, respectively, with a reduction of 5.05%. The data acquisition results show that part of the energy that would be lost could be stored in the DC bus. Changing the injection process could affect the energy gain considering that the amount of recovered energy depends directly on the braking regime of the machine.

It is effectively observed that the capacitor bank leads to reduced energy consumption since energy is stored for later use. There is no need for a rigid control of the DC bus voltage because the motor driver can handle voltage variations while observing safe operating limits for the semiconductor components. The variable-voltage DC bus associated with capacitor banks is a more efficient approach because the number of energy conversion stages is reduced. Besides, the process involves the direct energy exchange among the DC bus and machine drivers, as the current ripple of the PMSMs is reduced.

VII. CONCLUSION

This work has proposed a variable-voltage DC bus approach based on an energy recovery system for manufacturing industry applications, aiming at the efficient use of electric energy. A minimum value of the DC bus voltage is maintained to ensure the starting of motors. Besides, the DC bus voltage increased with the energy recovery process from the braking of motors until reaching a safe protection level. A capacitor bank was designed to allow exchanging energy with the bus. When the DC bus voltage increases, it is observed that the average current through it decreases. After carrying out computer simulations and laboratory tests with the capacitor bank connected to the system, field measurements were performed on a PVC injection molding machine in a footwear factory. The results were acquired with and without the capacitor bank connected to the DC bus to assess the performance of the energy storage system. Data acquired with an energy analyzer showed a reduction of 5% in the energy consumption when the capacitor bank was used. It means that the energy from the motor braking is stored in the DC bus and can be further used directly without the need for additional energy conversion stages, resulting in improved energy efficiency of the whole system.

REFERENCES

[1] B. A. Thomas, "Edison revisited: Impact of DC distribution on the cost of LED lighting and distributed generation," in *Proc. 25th Annu. IEEE Appl. Power Electron. Conf. Expo. (APEC)*, Feb. 2010, pp. 588–593, doi: 10.1109/APEC.2010.5433612.

[2] G. Ailee and W. Tschudi, "Edison redux," *IEEE Power Energy Mag.*, vol. 10, no. 6, pp. 50–59, Nov./Dec. 2012.

[3] P. Fairley, "DC versus AC: The second war of currents has already begun [in my view]," *IEEE Power Energy Mag.*, vol. 10, no. 6, pp. 103–104, Nov. 2012, doi: 10.1109/mpe.2012.2212617.

[4] P. Theisen, "A DC switching renaissance," in *Proc. 56th IEEE Holm Conf. Electr. Contacts*, Nov. 2010, p. 55, Accessed: Nov. 26, 2018. [Online]. Available: http://www.ieee-holm.org/h2010/h2010Theisen.pdf

[5] D. E. Geary. (2015). *Blinded by the Light' Visualizing the Future With Direct Current for Data Centers and DC Current Microgrids*. dcFUSION, LLC. Accessed: Nov. 26, 2018. [Online]. Available: http://www.apec-conf.org/wp-content/uploads/IS-13.5.pdf

[6] A. T. Elsayed, A. A. Mohamed, and O. A. Mohammed, "DC microgrids and distribution systems: An overview," *Electr. Power Syst. Res.*, vol. 119, pp. 407–417, Feb. 2015, doi: 10.1016/j.epsr.2014.10.017.

[7] H. Suryanarayana and S. D. Sudhoff, "Design paradigm for power electronics-based DC distribution systems," *IEEE J. Emerg. Sel. Topics Power Electron.*, vol. 5, no. 1, pp. 51–63, Mar. 2017, doi: 10.1109/JESTPE.2016.2626458.

[8] T. Dragičević, J. C. Vasquez, J. M. Guerrero, and D. Skrlec, "Advanced LVDC electrical power architectures and microgrids: A step toward a new generation of power distribution networks," *IEEE Electrific. Mag.*, vol. 2, no. 1, pp. 54–65, Mar. 2014, doi: 10.1109/MELE.2013.2297033.

[9] A. Maknouninejad, Z. Qu, F. L. Lewis, and A. Davoudi, "Optimal, nonlinear, and distributed designs of droop controls for DC microgrids," *IEEE Trans. Smart Grid*, vol. 5, no. 5, pp. 2508–2516, Sep. 2014, doi: 10.1109/TSG.2014.2325855.

[10] S. Augustine, M. K. Mishra, and N. L. Narasamma, "Proportional droop index algorithm for load sharing in DC microgrid," in *Proc. IEEE Int. Conf. Power Electron., Drives Energy Syst. (PEDES)*, Dec. 2014, pp. 1–6, doi: 10.1109/PEDES.2014.7042025.

[11] F. Nejabatkhah and Y. W. Li, "Overview of power management strategies of hybrid AC/DC microgrid," *IEEE Trans. Power Electron.*, vol. 30, no. 12, pp. 7072–7089, Dec. 2015, doi: 10.1109/TPEL.2014.2384999.

[12] T. Morstyn, B. Hredzak, and V. G. Agelidis, "Cooperative multi-agent control of heterogeneous storage devices distributed in a DC microgrid," *IEEE Trans. Power Syst.*, vol. 31, no. 4, pp. 2974–2986, Jul. 2016, doi: 10.1109/TPWRS.2015.2469725.

[13] M. Saeedifard, M. Graovac, R. F. Dias, and R. Iravani, "DC power systems: Challenges and opportunities," in *Proc. IEEE PES Gen. Meeting*, Jul. 2010, pp. 1–7, doi: 10.1109/PES.2010.5589736.

[14] D. J. Becker and B. J. Sonnenberg, "DC microgrids in buildings and data centers," in *Proc. IEEE 33rd Int. Telecommun. Energy Conf. (INTELEC)*, Oct. 2011, pp. 1–7, doi: 10.1109/INTLEC.2011.6099725.

[15] K. Garbesi, V. Vossos, and H. Shen, *Catalog of DC Appliances and Power Systems*. Berkeley, CA, USA: Lawrence Berkeley National Laboratory, Oct. 2012, pp. 1–77, doi: 10.2172/1076790.

[16] S. Moussa, M. J.-B. Ghorbal, and I. Slama-Belkhodja, "Bus voltage level choice for standalone residential DC nanogrid," *Sustain. Cities Soc.*, vol. 46, Apr. 2019, Art. no. 101431, doi: 10.1016/j.scs.2019.101431.

[17] A. S. Oliver. (2014). *Addressing 400-VDC Power in Advanced Industrial and Data-Center Apps*. Accessed: Dec. 5, 2018. [Online]. Available: http://www.powersystemsdesign.com/addressing-400-vdc-power-in-advanced-industrial-and-data-center-apps

[18] H. Kakigano, Y. Miura, and T. Ise, "Low-voltage bipolar-type dc microgrid for super high quality distribution," *IEEE Trans. Power Electron.*, vol. 25, no. 12, pp. 3066–3075, Dec. 2010, doi: 10.1109/TPEL.2010.2077682.

[19] M.-H. Ryu, H.-S. Kim, J.-W. Baek, H.-G. Kim, and J.-H. Jung, "Effective test bed of 380-V DC distribution system using isolated power converters," *IEEE Trans. Ind. Electron.*, vol. 62, no. 7, pp. 4525–4536, Jul. 2015, doi: 10.1109/TIE.2015.2399273.

[20] T. Dragicevic, X. Lu, J. Vasquez, and J. Guerrero, "DC mcrogrids—Part I: A review of control strategies and stabilization techniques," *IEEE Trans. Power Electron.*, vol. 31, no. 7, pp. 4876–4891, Jul. 2016, doi: 10.1109/TPEL.2015.2478859.

[21] T. Dragicevic, X. Lu, J. C. Vasquez, and J. M. Guerrero, "DC microgrids—Part II: A review of power architectures, applications, and standardization issues," *IEEE Trans. Power Electron.*, vol. 31, no. 5, pp. 3528–3549, May 2016, doi: 10.1109/TPEL.2015.2464277.

[22] J. P. Das, R. J. Fatema, and M. S. Anower, "Feasibility study of low voltage DC distribution system for residential buildings in bangladesh and hybrid home appliance design for tropical climate," in *Proc. 2nd Int. Conf. Electr., Comput. Telecommun. Eng. (ICECTE)*, Dec. 2016, pp. 8–10, doi: 10.1109/ICECTE.2016.7879625.

[23] R. Weiss, L. Ott, and U. Boeke, "Energy efficient low-voltage DC-grids for commercial buildings," in *Proc. IEEE 1st Int. Conf. DC Microgrids (ICDCM)*, Jun. 2015, pp. 154–158, doi: 10.1109/ICDCM.2015.7152030.

[24] L. E. Zubieta, "Demonstration of a microgrid based on a DC bus backbone at an industrial building," in *Proc. IEEE 2nd Int. Conf. DC Microgrids (ICDCM)*, Jun. 2017, pp. 235–241.

[25] R. Majumder, S. Auddy, B. Berggren, G. Velotto, P. Barupati, and T. U. Jonsson, "An alternative method to build DC switchyard with hybrid DC breaker for DC grid," *IEEE Trans. Power Del.*, vol. 32, no. 2, pp. 713–722, Apr. 2017, doi: 10.1109/TPWRD.2016.2582923.

[26] D. L. Gerber, V. Vossos, W. Feng, A. Khandekar, C. Marnay, and B. Nordman, "A simulation based comparison of AC and DC power distribution networks in buildings," in *Proc. IEEE 2nd Int. Conf. DC Microgrids (ICDCM)*, Jun. 2017, pp. 588–595, doi: 10.1109/ICDCM.2017.8001107.

[27] A. Ghazanfari and Y. A.-R. I. Mohamed, "Decentralized cooperative control for smart DC home with DC fault handling capability," *IEEE Trans. Smart Grid*, vol. 9, no. 5, pp. 5249–5259, Sep. 2018, doi: 10.1109/TSG.2017.2685562.

[28] Z. Shuai, J. Fang, F. Ning, and Z. J. Shen, "Hierarchical structure and bus voltage control of DC microgrid," *Renew. Sustain. Energy Rev.*, vol. 82, pp. 3670–3682, Feb. 2018, doi: 10.1016/j.rser.2017.10.096.

[29] V. Vossos, D. Gerber, Y. Bennani, R. Brown, and C. Marnay, "Techno-economic analysis of DC power distribution in commercial buildings," *Appl. Energy*, vol. 230, pp. 663–678, Nov. 2018, doi: 10.1016/j.apenergy.2018.08.069.

[30] D. Gerber, V. Vossos, and W. Feng, "A simulation-based efficiency comparison of AC and DC power distribution networks in commercial buildings," *Appl. Energy*, vol. 210, pp. 1167–1187, Jan. 2018, doi: 10.1016/j.apenergy.2017.05.179.

[31] D. L. Gerber, R. Liou, and R. Brown, "Energy-saving opportunities of direct-DC loads in buildings," *Appl. Energy*, vol. 248, pp. 274–287, Aug. 2019, doi: 10.1016/j.apenergy.2019.04.089.

[32] E. Rodriguez-Diaz, J. C. Vasquez, and J. M. Guerrero, "Intelligent DC homes in future sustainable energy systems: When efficiency and intelligence work together," *IEEE Consum. Electron. Mag.*, vol. 5, no. 1, pp. 74–80, Jan. 2016, doi: 10.1109/MCE.2015.2484699.

[33] M. Yuan, Y. Fu, Y. Mi, Z. Li, and C. Wang, "Hierarchical control of DC microgrid with dynamical load power sharing," *Appl. Energy*, vol. 239, pp. 1–11, Apr. 2019, doi: 10.1016/j.apenergy.2019.01.081.

[34] Y. Hahashi and M. Mino, "High-density bidirectional rectifier for next generation 380-V DC distribution system," in *Proc. 27th Annu. IEEE Appl. Power Electron. Conf. Expo. (APEC)*, Feb. 2012, pp. 2455–2460, doi: 10.1109/APEC.2012.6166166.

[35] X. F. Lin, Y. Z. Xue, C. N. Song, S. J. Song, and B. Liu, "An experiment and research platform for DC micro-grid," in *Proc. Chin. Control Conf. CCC*, Aug. 2016, pp. 8588–8595, doi: 10.1109/ChiCC.2016.7554727.

[36] U. Vuyyuru, S. Maiti, C. Chakraborty, and B. C. Pal, "A series voltage regulator for the radial DC microgrid," *IEEE Trans. Sustain. Energy*, vol. 10, no. 1, pp. 127–136, Jan. 2019.

[37] E. D. Queiroz and J. A. Pomilio, "PMSM drive system with variable DC bus for EV regenerative braking," in *Proc. 12th IEEE Int. Conf. Ind. Appl. (INDUSCON)*, Nov. 2016, pp. 1–8, doi: 10.1109/INDUSCON.2016.7874507.

[38] C.-Y. Yu, J. Tamura, and R. D. Lorenz, "Control method for calculating optimum DC bus voltage to improve drive system efficiency in variable DC bus drive systems," in *Proc. IEEE Energy Convers. Congr. Expo. (ECCE)*, Sep. 2012, pp. 2992–2999, doi: 10.1109/ECCE.2012.6342361.

[39] A. Bonanomi, (2016). *Electric Motors?: Market Trends and Service Business*. Power Transmission World. Accessed: Aug. 16, 2018. [Online]. Available: https://www.powertransmissionworld.com/electric-motors/

[40] P. Waide and C. Brunner, "Energy-efficiency policy opportunities for electric motor-driven systems," OECD Publishing, Paris, France, IEA Energy Papers 2011/07, 2011, doi: 10.1787/5kgg52gb9gjd-en.

[41] H. Ge, Y. Miao, B. Bilgin, B. Nahid-Mobarakeh, and A. Emadi, "Speed range extended maximum torque per ampere control for PM drives considering inverter and motor nonlinearities," *IEEE Trans. Power Electron.*, vol. 32, no. 9, pp. 1751–1759, 2017, doi: 10.1109/TPEL.2016.2630051.

[42] N. Kunihiro, K. Nishihama, M. Iizuka, K. Sugimoto, and M. Sawahata, "Investigation into loss reduced rotor slot structure by analyzing local behaviors of harmonic magnetic fluxes in inverter-fed induction motor," *IEEE Trans. Ind. Appl.*, vol. 53, no. 2, pp. 1070–1077, Mar. 2017, doi: 10.1109/TIA.2016.2642481.

[43] M. Melfi, "Quantifying the energy efficiency of motors on inverters," *IEEE Ind. Appl. Mag.*, vol. 17, no. 6, pp. 37–43, Nov. 2011, doi: 10.1109/MIAS.2011.942301.

[44] C. Laoufi, A. Abbou, and M. Akherraz, "Comparative study between several strategies speed controllers in an indirect field-oriented control of an induction machine," in *Proc. Int. Renew. Sustain. Energy Conf. (IRSEC)*, Oct. 2014, pp. 866–872, doi: 10.1109/IRSEC.2014.7059776.

[45] S. Hussain and M. A. Bazaz, "Comparative analysis of speed control strategies for vector controlled PMSM drive," in *Proc. Int. Conf. Comput., Commun. Autom. (ICCCA)*, Apr. 2016, pp. 1314–1319, doi: 10.1109/CCAA.2016.7813950.

[46] X. Lu, J. Guerrero, R. Teodorescu, T. Kerekes, K. Sun, and L. Huang, "Control of parallel-connected bidirectional AC–DC converters in stationary frame for microgrid application," in *Proc. IEEE Energy Convers. Congr. Expo.*, Sep. 2011, pp. 4153–4160, doi: 10.1109/ECCE.2011.6064335.

[47] Y. Hayashi and M. Mino, "A new approach to higher density rectifier with SiC power devices for 380 V DC distribution systems," in *Proc. 14th Eur. Conf. Power Electron. Appl. (EPE)*, Sep. 2011, pp. 1–8.

[48] P. Meng, Z. Jian, L. Wenshan, and W. Youlong, "The study and application of CAN communication of rectifier parallel operation control system," in *Proc. 19th Int. Conf. Electr. Mach. Syst.*, Nov. 2016, pp. 1–4.

[49] Z. Cao, H. Fahnert, J. Schiele, J. Solanki, N. Froehleke, and J. Boecker, "System concept and model-based optimization of high-current variable-voltage chopper-rectifiers," in *Proc. PCIM Eur., Int. Exhib. Conf. Power Electron., Intell. Motion, Renew. Energy Energy Manage.*, 2016, pp. 1–7.

[50] K. Kumar, "Efficiency improvement of three phase traction inverter through GaN devices for PMSM," in *Proc. IEEE Int. Conf. Power Electron., Drives Energy Syst. (PEDES)*, Dec. 2016, pp. 1–6, doi: 10.1109/PEDES.2016.7914359.

[51] D. P. Nam, P. T. Thanh, and T. X. Tinh, "Output feedback controller using high-gain observer in multi-motor drive systems," in *Proc. Int. Conf. Syst. Sci. Eng. (ICSSE)*, Jul. 2017, pp. 428–431, doi: 10.1109/ICSSE.2017.8030911.

[52] J. Li, T. Tang, T. Wang, and G. Yao, "Modeling and simulation for common DC bus multi-motor drive systems based on activity cycle diagrams," in *Proc. IEEE Int. Symp. Ind. Electron.*, Jul. 2010, pp. 250–255, doi: 10.1109/ISIE.2010.5637567.

[53] O. Gottberg, J. Kajaste, T. Minav, H. Kauranne, O. Calonius, and M. Pietola, "Energy balance of electro-hydraulic powertrain in a micro excavator," in *Proc. Global Fluid Power Soc. PhD Symp. (GFPS)*, Jul. 2018, pp. 1–6, doi: 10.1109/GFPS.2018.8472368.

[54] T. Minav, H. Hänninen, A. Sinkkonen, L. Laurila, and J. Pyrhönen, "Electric or hydraulic energy recovery systems in a reach truck—A comparison," *Strojniški Vestnik J. Mech. Eng.*, vol. 60, no. 4, pp. 232–240, Apr. 2014, doi: 10.5545/sv-jme.2013.1581.

[55] T. A. Minav, J. J. Pyrhonen, and L. I. E. Laurila, "Permanent magnet synchronous machine sizing: Effect on the energy efficiency of an electro-hydraulic forklift," *IEEE Trans. Ind. Electron.*, vol. 59, no. 6, pp. 2466–2474, Jun. 2012, doi: 10.1109/TIE.2011.2148682.

[56] G. Hu, A. Xia, Z. Li, X. Mei, and F. Wang, "Research on injection molding machine drive system based on model predictive control," in *Proc. 2nd Int. Conf. Robot. Autom. Eng. (ICRAE)*, Dec. 2017, pp. 161–167, doi: 10.1109/ICRAE.2017.8291373.

[57] I. Karatzaferis, E. C. Tatakis, and N. Papanikolaou, "Investigation of energy savings on industrial motor drives using bidirectional converters," *IEEE Access*, vol. 5, pp. 17952–17961, 2017, doi: 10.1109/ACCESS.2017.2748621.

[58] K. Takahashi, M. Okamoto, E. Hiraki, and T. Tanaka, "Simulation analysis of energy-saving effect of an energy recovery system for electric motor drive system in the injection molding machine," in *Proc. 14th Int. Power Electron. Motion Control Conf. (EPE-PEMC)*, Sep. 2010, pp. 118–122, doi: 10.1109/EPEPEMC.2010.5606863.

[59] H. Akiyoshi, E. Hiraki, T. Tanaka, M. Okamoto, T. Matsuo, and K. Ochi, "Peak power shaving of an electric injection molding machine with supercapacitors," *IEEE Trans. Ind. Appl.*, vol. 50, no. 2, pp. 1114–1120, Mar. 2014, doi: 10.1109/TIA.2013.2272433.

ANDRE DOS SANTOS LIMA (Graduate Student Member, IEEE) received the B.Sc. degree in electrical engineering from the University of Fortaleza, in 1993, the master's degree in electrical engineering from the Federal University of Ceará, Sobral, in 2008, where he is currently pursuing the Ph.D. degree. Since 2009, he has been an Assistant Professor of electrical engineering with the Federal University of Ceará. He worked with OI (Telemar Norte Leste S/A), a big Brazilian telecom company, almost ten years, in many areas, such as telecom network maintenance, financial, IT, and marketing. He has experience in power electronics, with emphasis on electronic circuits, working mainly on the following topics, such as direct current buses, power converters, three-phase rectifier, system photovoltaic, vibratory pump, and power factor.

ADERALDO RICARTE GUEDES received the B.Sc. degree in computer engineering from the Federal University of Ceará–Campus Sobral in 2010, the B.Sc. degree in industrial mechatronics from the Federal Institute of Ceara in 2011, the Specialization degree in work security and environmental management from Candido Mendes University in 2018, and the master's degree in electrical engineering and computer from the Federal University of Ceara in 2018, where he is currently pursuing the Ph.D. degree. He is an employee at Grendene S/A and a Technical Accessor of CNTT NR-12 of National Confederation of Industry-DF. He focused mainly in the subjects are DC BUS, power efficiency, recovering of break energy, Supercapacitor, and voltage levels.

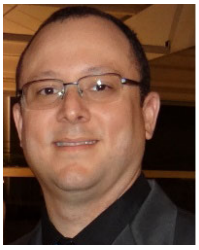

EDILSON MINEIRO SA JUNIOR was born in Fortaleza, Brazil. He received the B.Sc. and M.S. degrees in electrical engineering from the Federal University of Ceará, Fortaleza, in 1999 and 2004, respectively, and the Ph.D. degree from the Federal University of Santa Catarina, Florianopolis, Brazil, in 2010. Since 2008, he has been a Professor with the Federal Institute of Ceará, Sobral, Brazil, where he coordinates the Mechatronics Research Group (GPEM). In 2017, he won the Award for Best Paper at the IEEE/PELS International Conference PEDG2017 (The 8th International Symposium on Power Electronics for Distributed Generation Systems). His research interests include electronic ballasts, power factor correction circuits, dc–dc converters and their application to renewable energy systems, and LED drivers. He is a member of the Brazilian Power Electronics Society (SOBRAEP). He is a Reviewer of the following journals, such as *IET Electronics Letters*, IEEE TRANSACTIONS ON INDUSTRIAL ELECTRONICS, IEEE TRANSACTIONS ON INDUSTRIAL APPLICATION, IEEE TRANSACTIONS ON POWER ELECTRONICS, *International Transactions on Electrical Energy Systems*, and *International Journal of Electronics and Power Electronics Magazine* (SOBRAEP).

FERNANDO LUIZ MARCELO ANTUNES (Member, IEEE) received the B.Sc. degree in electrical engineering from the Federal University of Ceará, Brazil, the B.Sc. degree in business and administration from the State University of Ceará, Brazil, the M.Sc. degree from the University of São Paulo, Brazil, and the Ph.D. degree from the Loughborough University of Technology, U.K.,1991. He is currently a Full Professor with the Federal University of Ceará, where he is doing research in power electronics, renewables, and LED drivers. His research interests include multilevel converters and DC microgrids. He is a member of the IEEE Societies Power Electronics (PELS), the Industrial Electronics Society, and the IE and Power Engineering (PES). He is a Member Former President of the Brazilian Power Electronics Society (SOBRAEP).